

Supporting Information for:

Kinetics and mechanism of OH-mediated degradation of three pentanols in the atmosphere

Feng-Yang Bai,^{a*} Mei-Yan Chen,^a Xiang-Huan Liu,^a Shuang Ni,^{a,b} Yi-Zhen Tang,^c
Xiu-Mei Pan,^b Zhen Zhao,^{a,d*}

^a*Institute of Catalysis for Energy and Environment, College of Chemistry and Chemical Engineering,
Shenyang Normal University, Shenyang, 110034, People's Republic of China*

^b*National & Local United Engineering Lab for Power Battery, Faculty of Chemistry, Northeast Normal
University, Changchun, 130024, People's Republic of China*

^c*Department of Chemistry, School of Environmental and Municipal Engineering, Qingdao
Technological University, Qingdao, 266033, People's Republic of China*

^d*State Key Laboratory of Heavy Oil Processing, China University of Petroleum, Chang Ping,
Beijing 102249, People's Republic of China*

*Corresponding author: baify492@nenu.edu.cn (Feng-Yang Bai)

*Corresponding author: zhenzhao@cup.edu.cn (Zhen Zhao)

S1. Details of rate constant calculations.

The multistructural method with coupled torsional-potential anharmonicity¹ (MS-T) was used for calculating partition functions by the MSTor-2017-B.² Then, we carried out first-principles direct dynamics calculations using multistructural canonical variational transition state theory with small curvature tunneling (MS-CVT/SCT)³ to calculate the high-pressure-limit rate constants of reaction channels RA1–RA6, RB1–RB6 and RC1–RC4. For the current system which contains one chiral carbon, we followed the procedures in the previous paper⁵⁶ for treating chiral centers in MS-VTST theory.

The CVT rate coefficient at temperature T was computed by

$$k^{CVT}(T) = \min k^{GT}(T, s) \quad (1)$$

$$k^{GT}(T, s) = \frac{\sigma \kappa k_B T Q^{GT}(T, s)}{h Q^R(T)} \exp\left(-\frac{V_{MEP}(s)}{k_B T}\right) \quad (2)$$

Herein, s is the location of the generalized transition state on the IRC; σ is the symmetry factor; k_B is Boltzmann's constant; h is Planck's constant; κ is the tunneling factor; and Q^{GT} and Q^R are partition functions for the generalized transition state and reactants, respectively. In the computations of the electronic partition functions, two electronic states for OH radical, with a 140 cm^{-1} splitting in the ${}^2\Pi_{1/2}$ and ${}^2\Pi_{3/2}$ ground states, are included. The vibrationally adiabatic ground-state energy, which is the effective potential for tunneling, is given by

$$V_a^G = V_{MEP}(s) + \varepsilon^G(s) \quad (3)$$

where s is the reaction coordinate, which is a signed distance from the saddle point along each curved MEP in isoinertial coordinates, $V_{MEP}(s)$ is the potential energy along the MEP, and $\varepsilon^G(s)$ is the local zero-point energy.

The MS-VTST rate constants were calculated by³

$$k^{CVT/SCT} = F_{act}^{MS-T} k_1^{CVT/SCT} \quad (4)$$

where $k_1^{CVT/SCT}$ is the single-structural canonical variation theory⁴ (CVT) rate constant SCT approximation,^{5,6} which employs the lowest-energy structure (labeled as 1 here) for reactants and the transition state. F_{act}^{MS-T} is the multistructural torsional anharmonicity factor of the reaction: it includes the contributions from all the conformational structures of the reactants and the transition state and is computed by the coupled-potential MS-T method as described elsewhere.⁷⁻¹⁰ It is calculated by

$$F_{act}^{MS-T} = F_{TS}^{MS-T} / F_R^{MS-T} \quad (5)$$

where F_X^{MS-T} is the multistructural torsional anharmonicity factor of species X, and it equals the ratio of the MS-T partition function to the single-structure harmonic one. As in the original MS-VTST method, F_{TS}^{MS-T} was approximated by its value at the conventional transition state. In the MS-T method, the potential for the torsional coordinate $\phi_{j,\tau}$ of torsion τ of structure j of a given species is approximated locally as

$$V_{j,\tau} = U_j + A_{j,\tau} [1 - \cos M_{j,\tau} (\phi_{j,\tau} - \phi_{j,\tau,eq})] \quad (6)$$

where U_j is the energy of the structure, $\phi_{j,\tau,eq}$ is the equilibrium value of the torsion angle, $M_{j,\tau}$ is the local periodicity, determined by Voronoi tessellation, and $A_{j,\tau}$ is determined from the second-order force constants and the local periodicities.¹ Effects caused by the deviation of eq. 6 from a harmonic potential are called torsional potential anharmonicity effects; the effect of including the contributions of all the distinguishable structures of a species (a reactant species or a transition state) is called multiple-structure anharmonicity. The combination of these two effects is called multi-structural anharmonicity.

References

1. J. J. Zheng, D. G. Truhlar, *J. Chem. Theory Comput.* 2013, **9**, 1356–1367.
2. J. J. Zheng, S. L. Mielke, J. L. Bao, R. Meana-Pañeda, K. L. Clarkson, D. G. Truhlar, *University of Minnesota: Minneapolis*, MN. 2017.
3. T. Yu, J. J. Zheng, D. G. Truhlar, *Chem. Sci.* 2011, **2**, 2199–2213.
4. Garrett, B. C.; Truhlar, D. G. *J. Chem. Phys.* 1979, **70**, 1593–1598.
5. Liu, Y. P.; Lynch, G. C.; Truong, T. N.; Lu, D. H.; Truhlar, D. G.; Garrett, B. C. *J. Am. Chem. Soc.* 1993, **115**, 2408–2415.
6. D. G. Truhlar, R. S. Grev, A. W. Magnuson, *J. Phys. Chem.* 1980, **84**, 1730–1748.
7. J. L. Bao, J. J. Zheng, D. G. Truhlar, *J. Am. Chem. Soc.* 2016, **138**, 2690–2704.
8. J. L. Bao, Zhang, X.; Truhlar, D. G. *Phys. Chem. Chem. Phys.* 2016, **18**, 16659–16670.
9. Bao, J. L.; Truhlar, D. G. *Phys. Chem. Chem. Phys.* 2016, **18**, 10097–10108.
10. Bao, J. L.; Sripa, P.; Truhlar, D. G. *Phys. Chem. Chem. Phys.* 2016, **18**, 1032–1041.

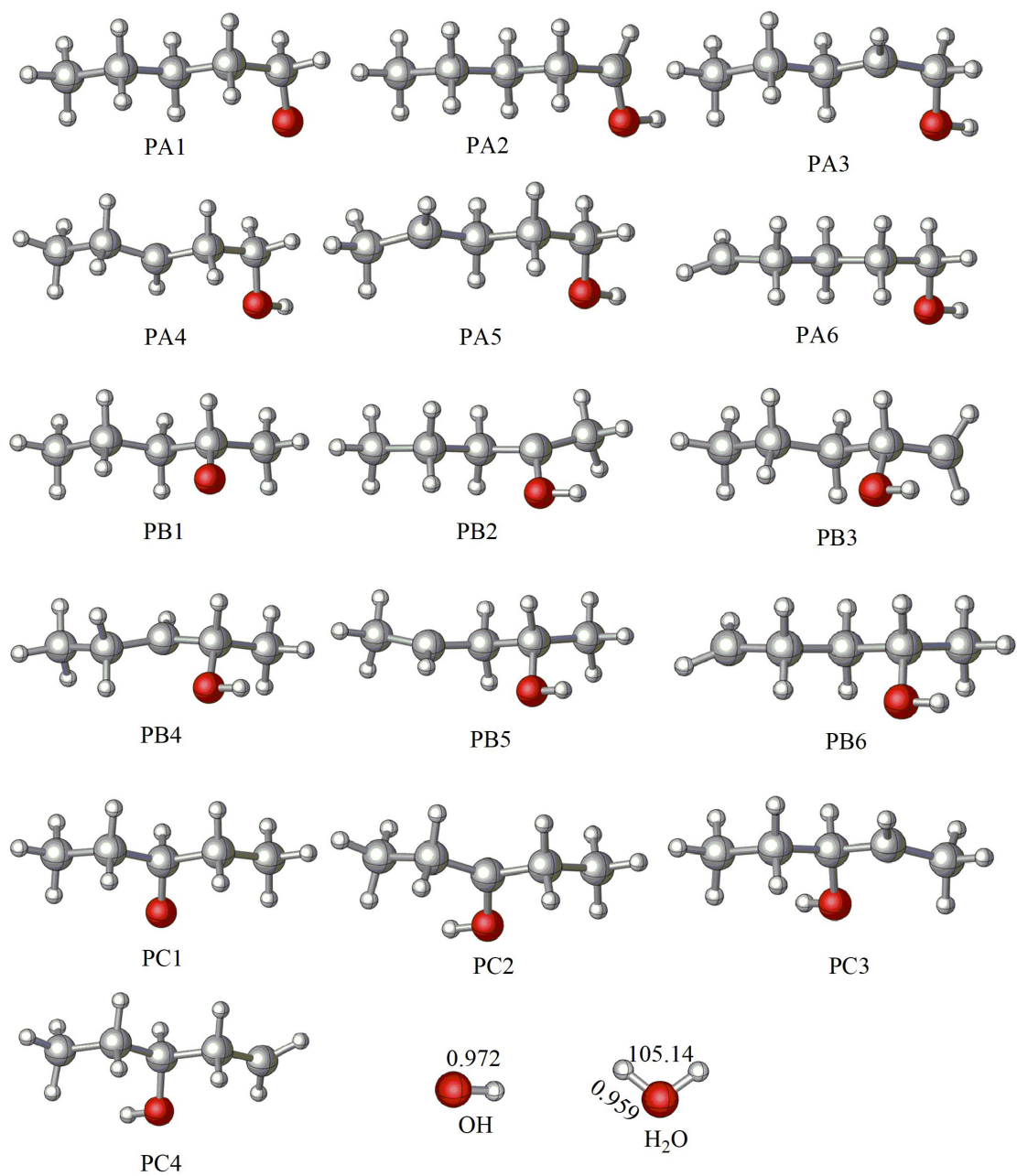


Figure S1. The geometries of the OH, H₂O, and hydrogen abstraction products involving the initial reactions of 1-pentanol (A), 2-pentanol (B), and 3-pentanol (C) with OH radical at the M06-2X/6-311+G(d,p) level.

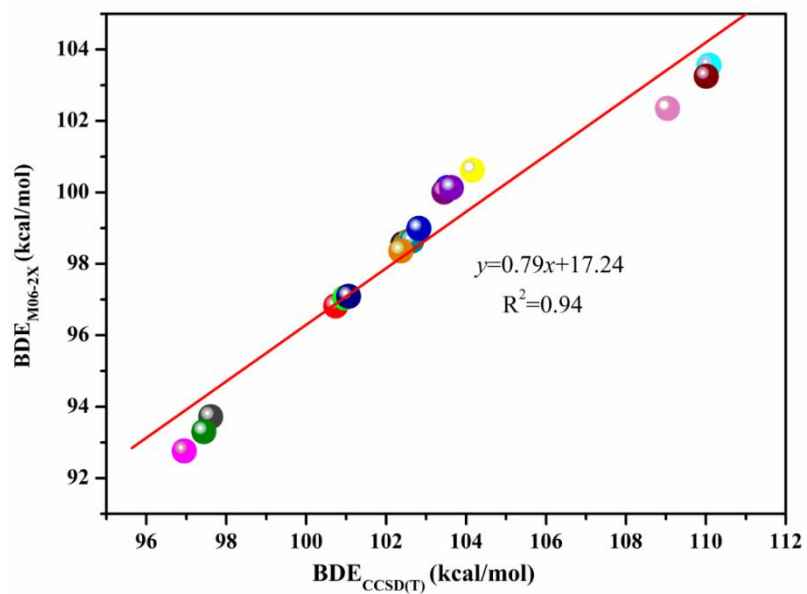


Figure S2. Plots of C–H (O–H) BDE obtained at the M06-2X/6-311+G(d,p) level versus C–H (O–H) BDE obtained at the CCSD(T)/CBS//M06-2X/6-311+G(d,p) level.

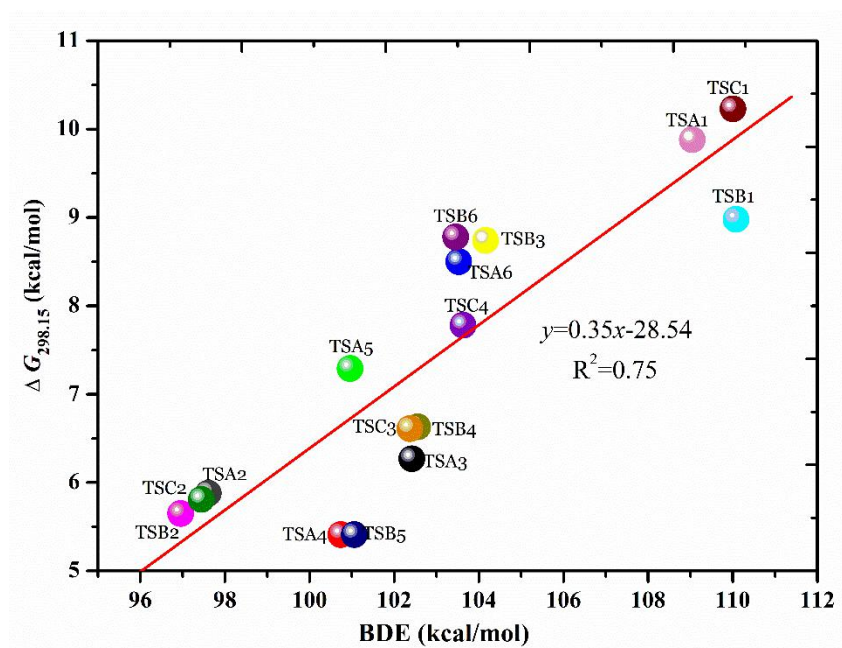


Figure S3. Plots of relative free energies ($\Delta G_{298.15}$) versus C–H (O–H) BDE at the CCSD(T)/CBS//M06-2X/6-311+G(d,p) level.

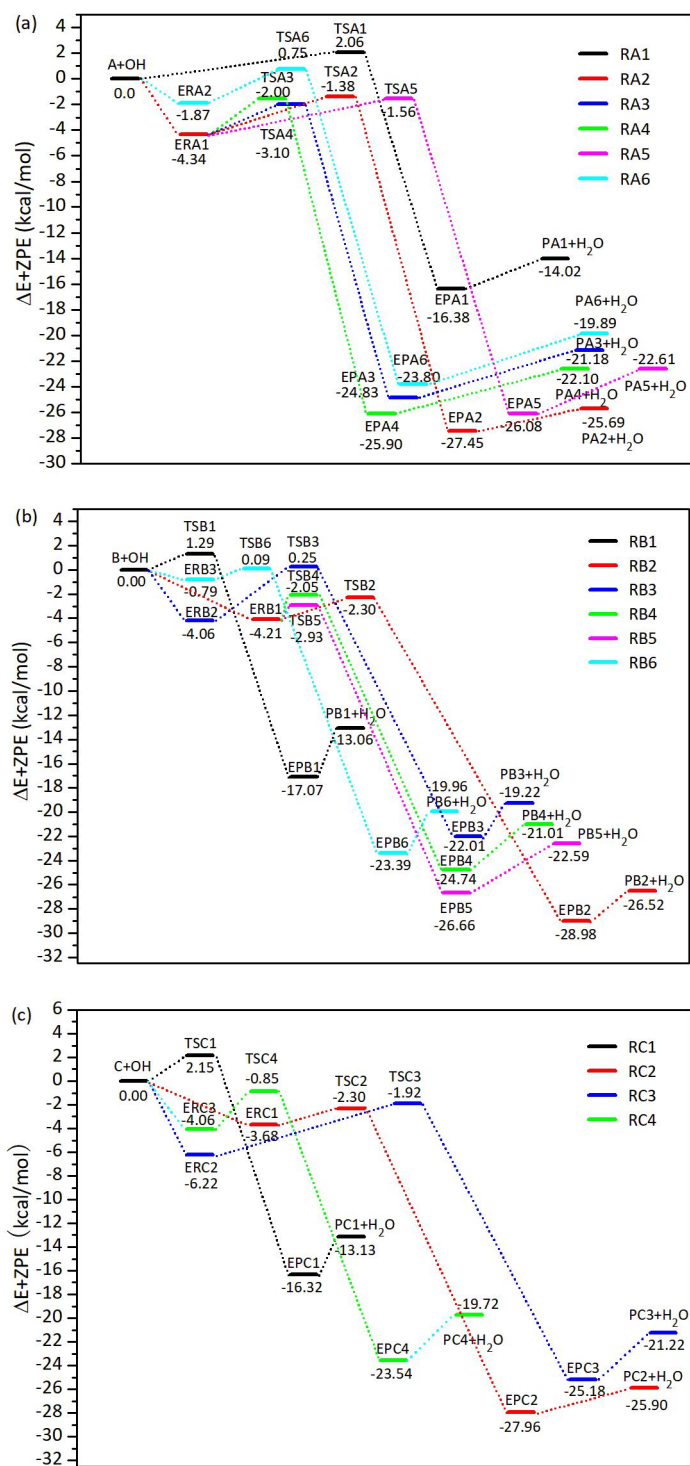


Figure S4. Schematic potential energy surfaces for reactions of 1-pentanol (A) + OH (a), 2-pentanol (B) + OH (b), and 3-pentanol (C) + OH (c). The relative energies are calculated at the CCSD(T)/CBS//M06-2X/6-311+G(d,p) level.

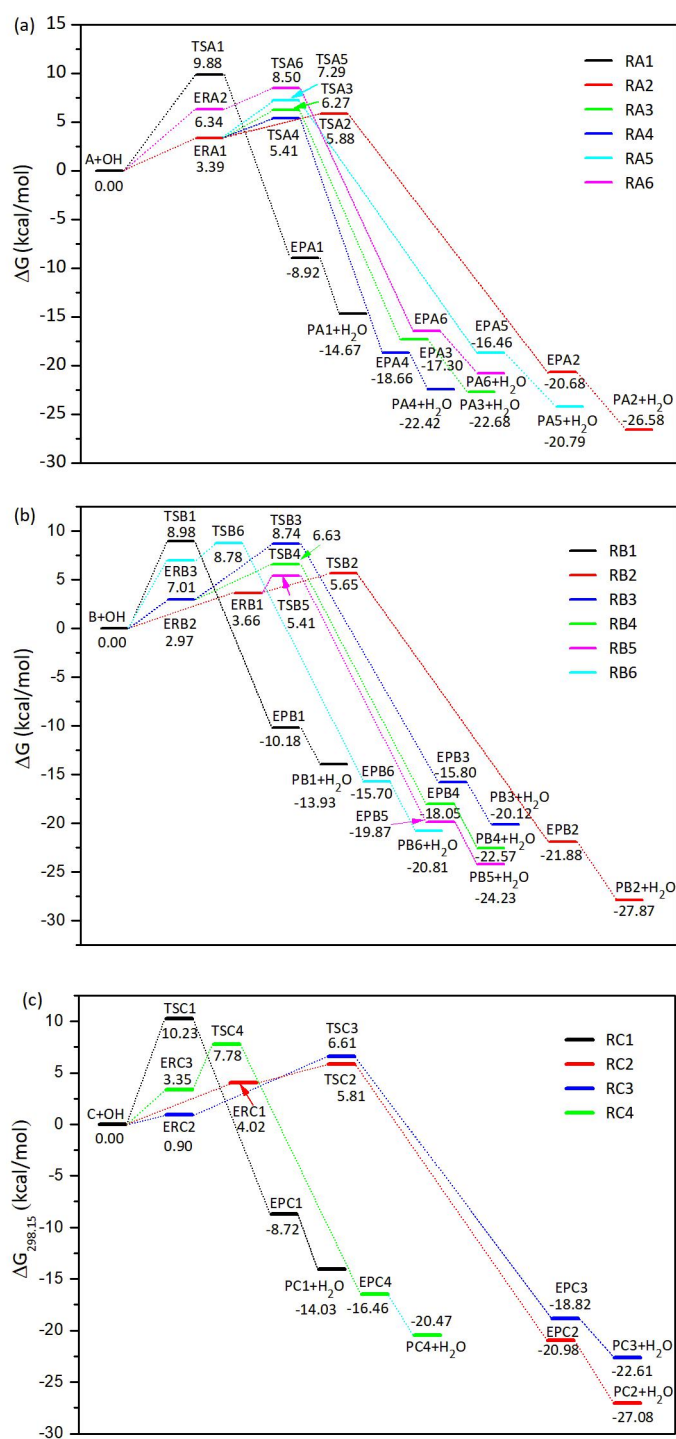


Figure S5. Schematic free energy surfaces (at 298.15 K) for reactions of 1-pentanol (A) + OH (a), 2-pentanol (B) + OH (b), and 3-pentanol (C) + OH (c). The relative energies are calculated at the CCSD(T)/CBS//M06-2X/6-311+G(d,p) level.

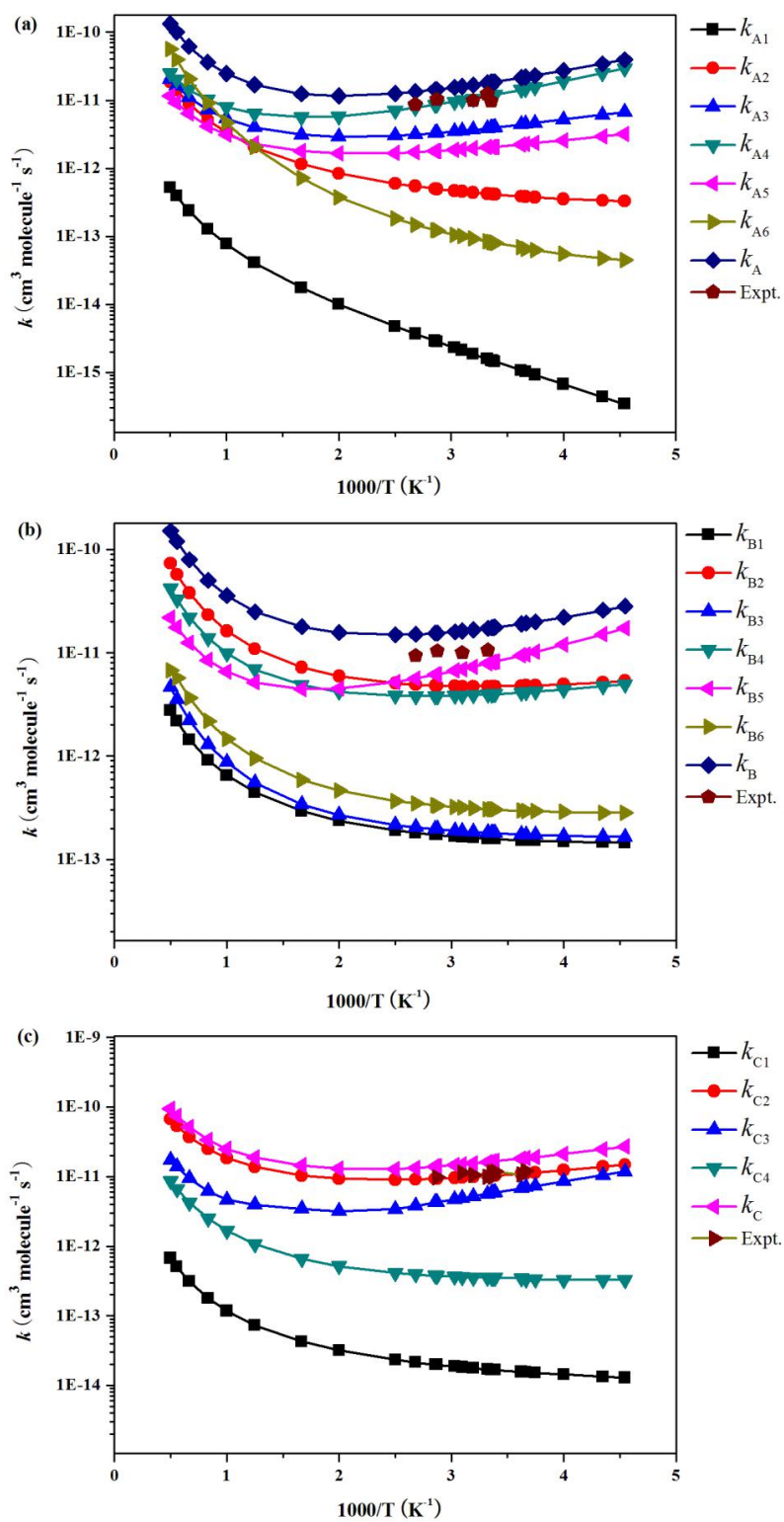


Figure S6. CCSD(T)/CBS//M06-2X/6-311+G(d,p)-computed individual and total MS-CVT/SCT rate constants versus $1000/T$ together with the experimental data for reactions of RA1–RA6 (a), RB1–RB6 (b), and RC1–RC6 (c) in the temperature range of 220–2000 K.

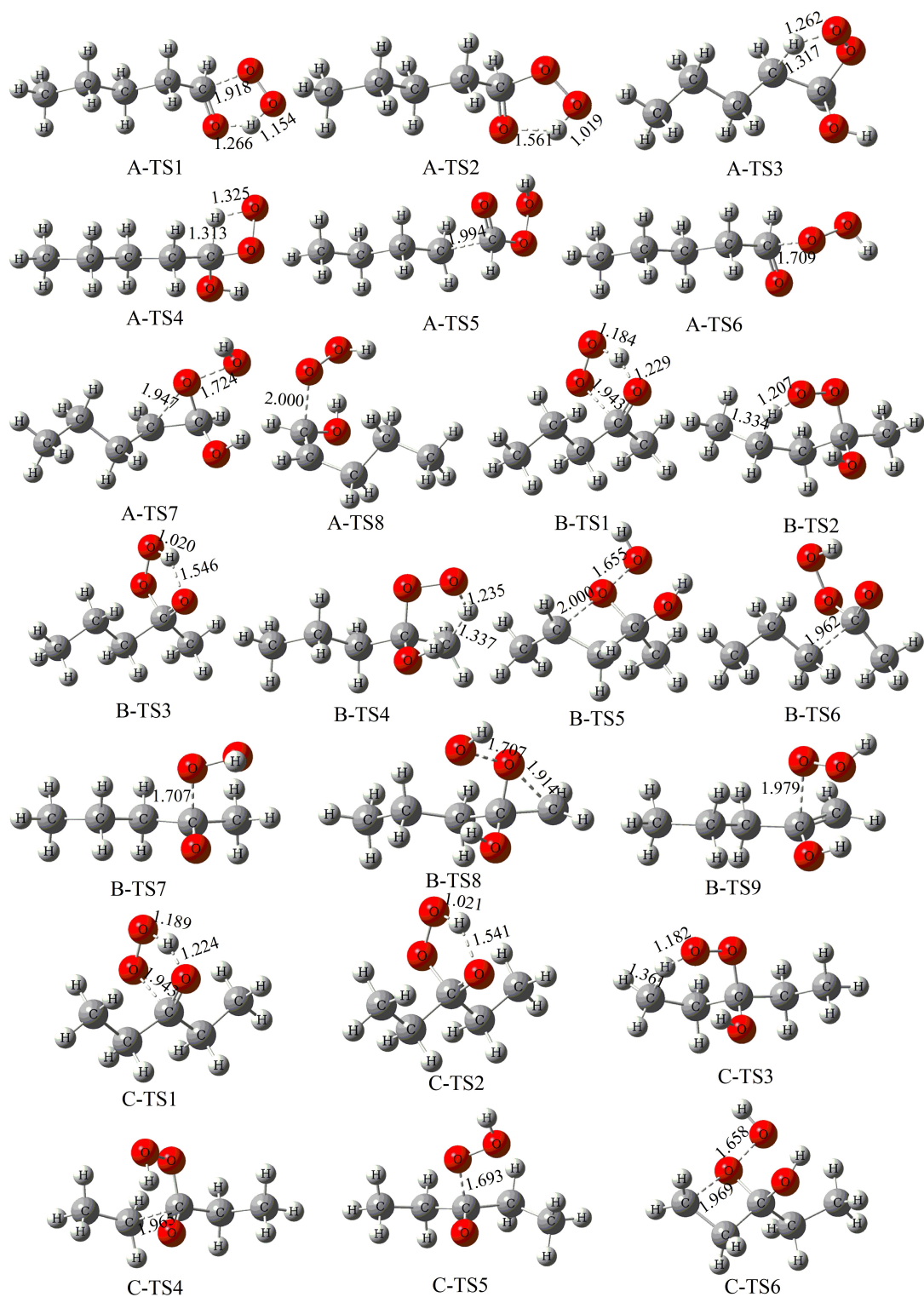


Figure S7. The geometries for the transition states in gaseous phase in the subsequent degradation of peroxy radicals.

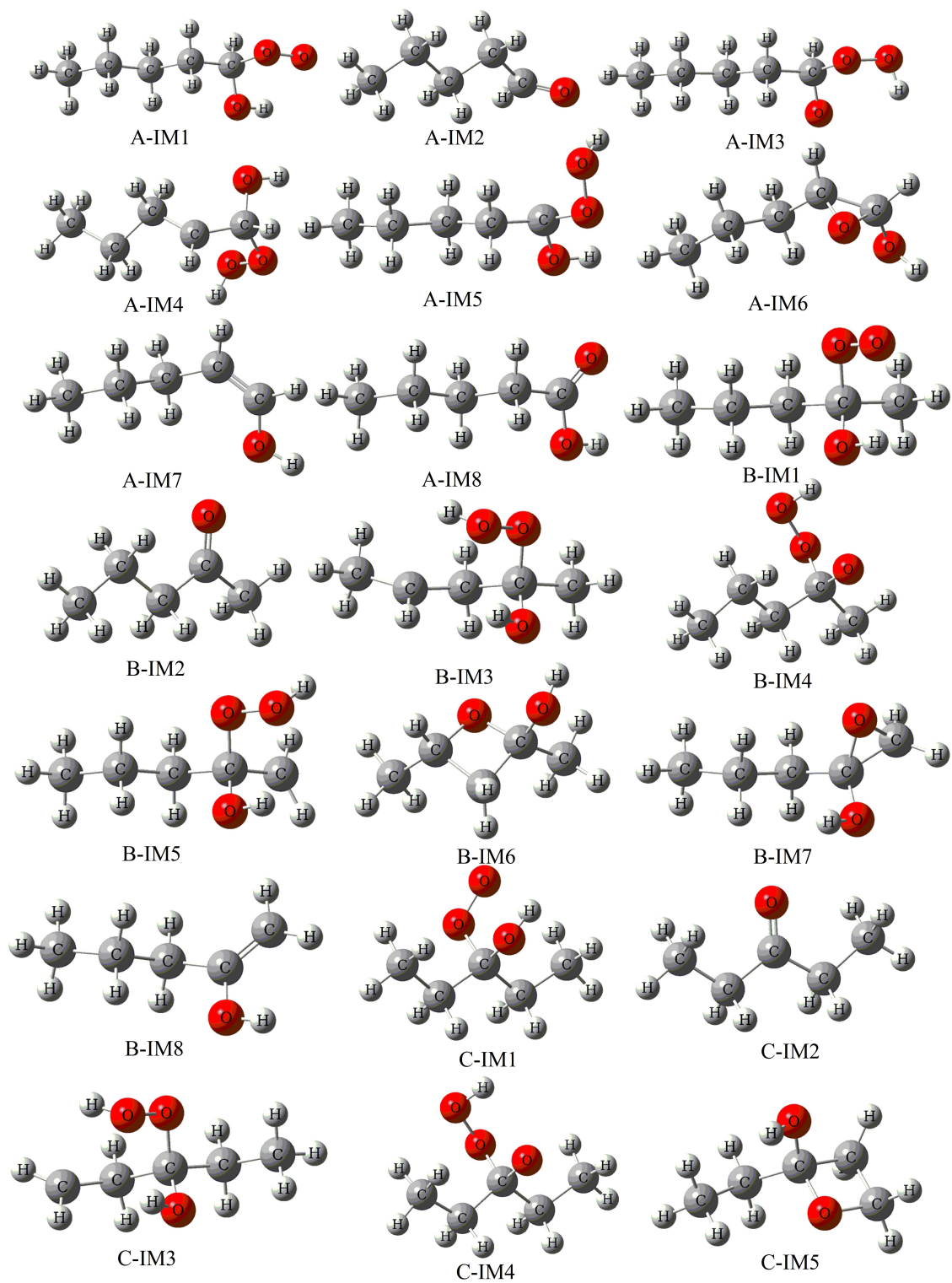


Figure S8. The geometries for the stationary points in gaseous phase in the subsequent degradation of peroxy radicals.

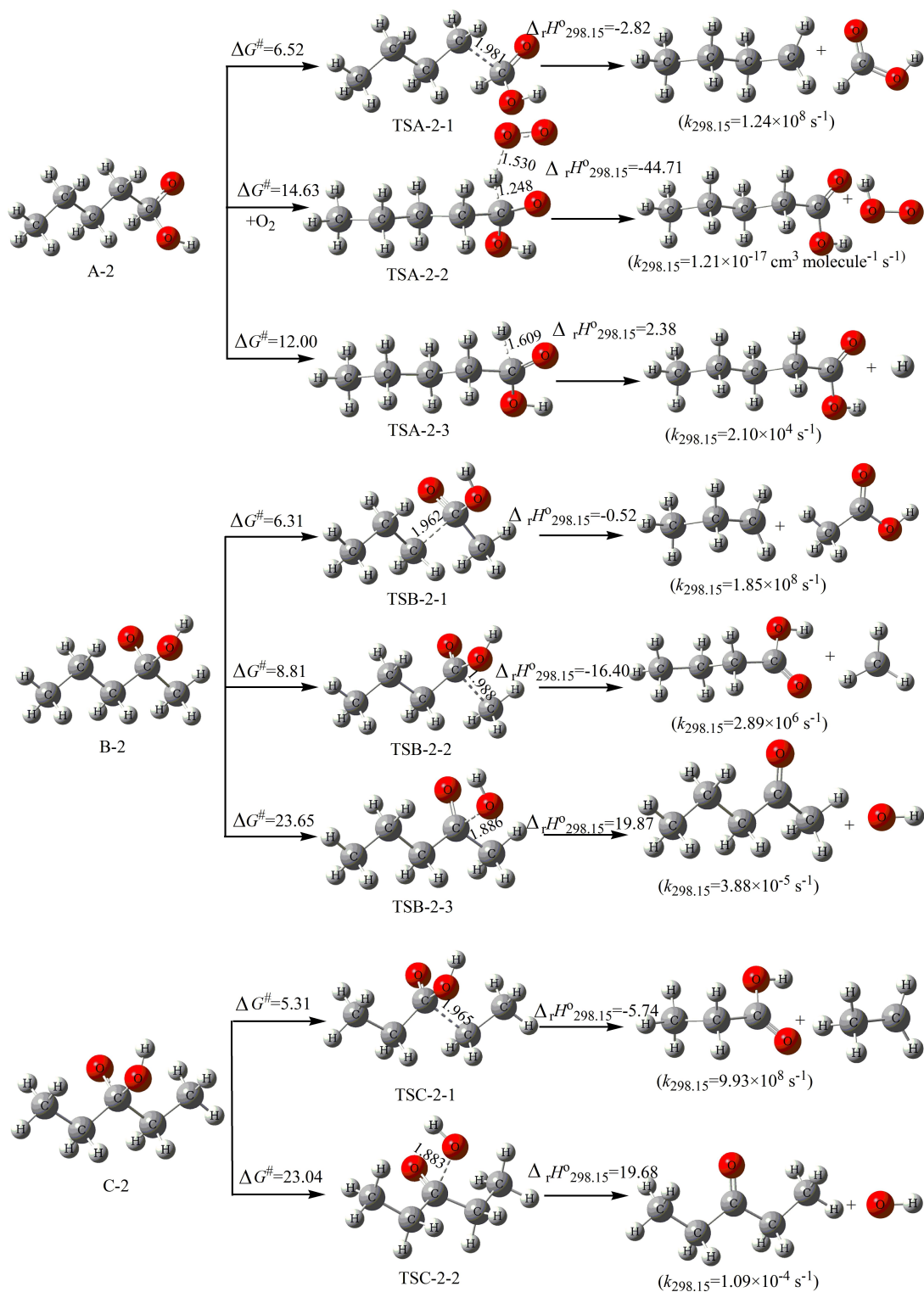


Figure S9. The degradation pathways along with the geometrical configurations of hydroxyalkoxy radicals A-2, B-2, and C-2.

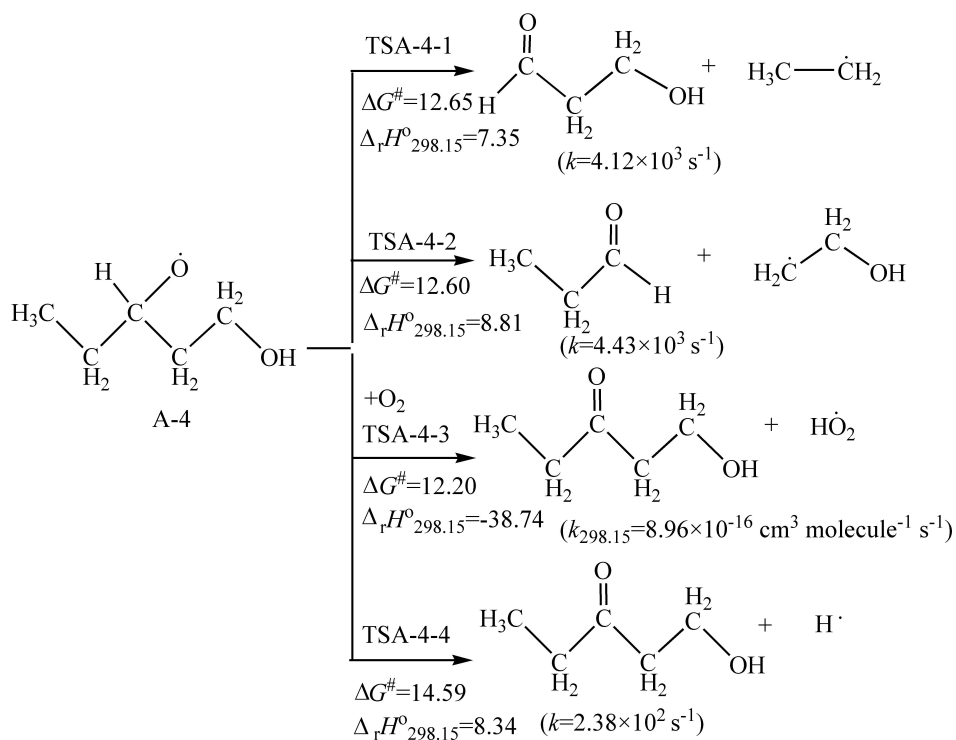
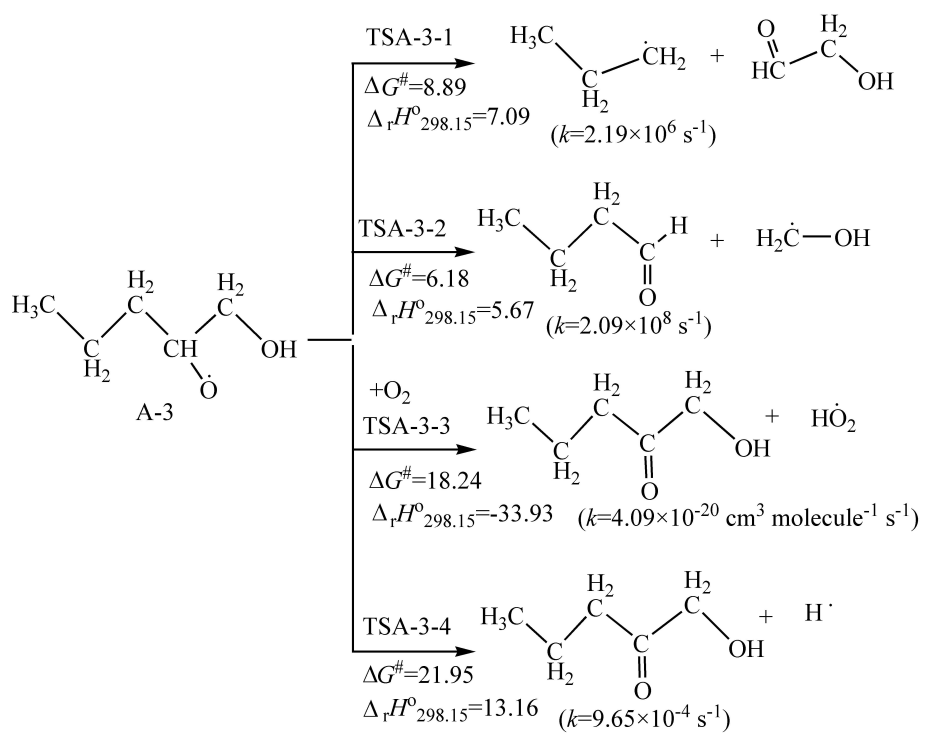


Figure S10. The transformation pathways and fate of hydroxyalkoxy radicals A-3 and A-4 in the presence of O₂.

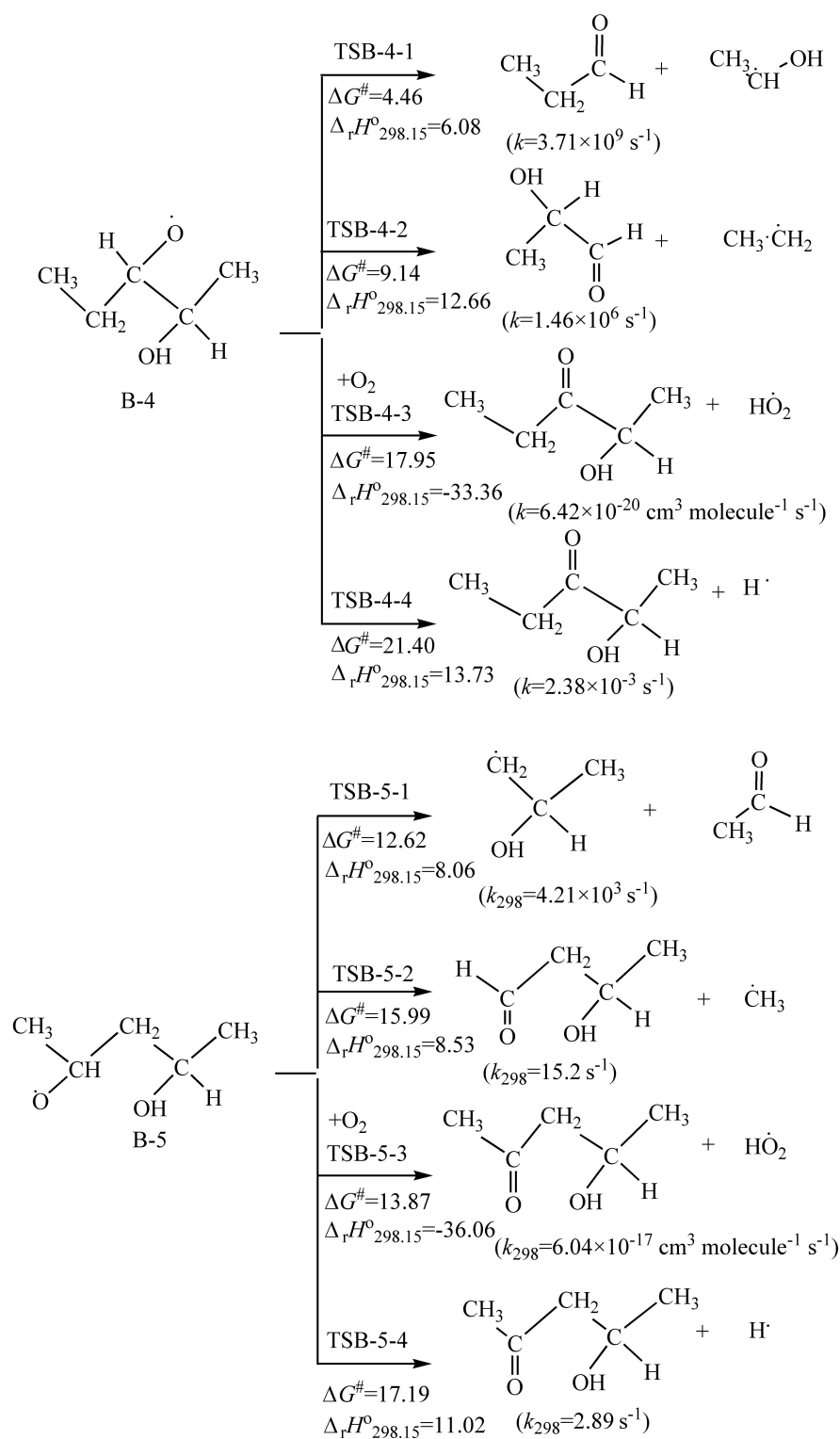


Figure S11. The transformation pathways and fate of hydroxyalkoxy radicals B-4 and B-5 in the presence of O₂.

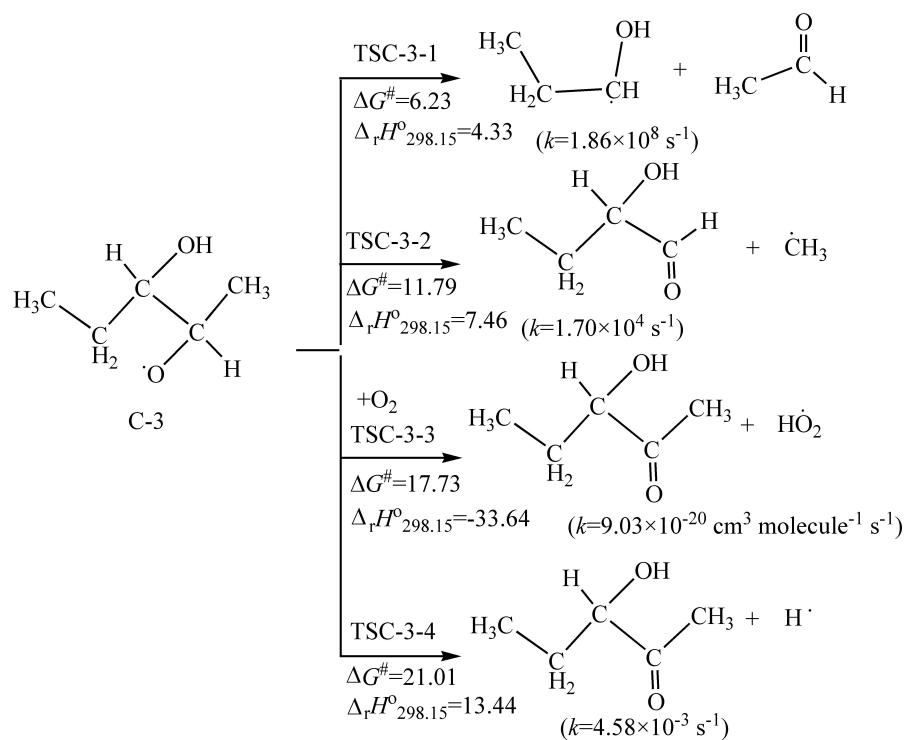


Figure S12. The transformation pathways and fate of hydroxyalkoxy radicals C-3 in the presence of O₂.

Table S1. The interaction energy (ΔE_{inter}) and the total distortion energy (ΔE_{d}) (kcal/mol) for all hydrogen abstraction transition states at the M06-2X/6-311+G(d,p) level.

Species	ΔE_{d}	ΔE_{inter}
TSA1	5.72	-3.90
TSA2	1.35	-1.96
TSA3	2.96	-4.53
TSA4	2.64	-5.51
TSA5	4.72	-6.32
TSA6	2.38	0.52
TSB1	5.14	-4.42
TSB2	1.19	-3.16
TSB3	4.48	-3.55
TSB4	2.85	-4.91
TSB5	2.80	-5.19
TSB6	5.91	-5.68
TSC1	6.04	-4.35
TSC2	1.19	-3.55
TSC3	2.89	-4.55
TSC4	3.96	-4.57

Table S2. Relative energies ($\Delta E_{298.15}$), standard Enthalpies change ($\Delta H_{298.15}$), and Gibbs free energy change ($\Delta G_{298.15}$) of reactant complexes and transition states in the reactions of OH radical with 1-pentanol (A), 2-pentanol (B), and 3-pentanol (C) at the CCSD(T)/CBS//M06-2X/6-311G(d,p) level.

Species	$\Delta E_{298.15}$	$\Delta H_{298.15}$	$\Delta G_{298.15}$
A + OH	0.0	0.0	0.0
ERA1	-4.34	-4.88	3.39
ERA2	-1.87	-2.48	6.34
TSA1	2.06	1.25	9.88
TSA2	-1.38	-2.03	5.88
TSA3	-2.00	-2.95	6.27
TSA4	-3.10	-4.12	5.41
TSA5	-1.56	-2.66	7.29
TSA6	0.75	-0.03	8.50
B + OH	0.0	0.0	0.0
ERB1	-4.21	-4.61	2.97
ERB2	-4.06	-4.56	3.66
ERB3	-0.79	-1.25	7.01
TSB1	1.29	0.52	8.98
TSB2	-2.30	-3.00	5.65
TSB3	0.25	0.74	8.74
TSB4	-2.05	-3.04	6.63
TSB5	-2.93	-3.86	5.41
TSB6	0.09	-1.02	8.78
C + OH	0.0	0.0	0.0
ERC1	-3.68	-4.25	4.02
ERC2	-4.56	-4.89	2.64
ERC3	-6.23	-6.68	0.90
ERC4	-4.06	-4.49	3.35
TSC1	2.15	1.37	10.23
TSC2	-2.30	-3.06	5.81
TSC3	-1.92	-2.83	6.61
TSC4	-0.85	-1.97	7.78

Table S3. Calculated MS-CVT/SCT rate constants ($\text{cm}^3 \text{ molecule}^{-1} \text{ s}^{-1}$) for reactions of A/B/C + OH in the temperature range of 220–2000 K at CCSD(T)/CBS//M06-2X/6-311+G(d,p) level.

T (K)	k_A	k_B	k_C
220	3.96E-11	2.82E-11	2.70E-11
230	3.44E-11	2.56E-11	2.47E-11
250	2.72E-11	2.20E-11	2.12E-11
267	2.30E-11	1.98E-11	1.91E-11
273	2.19E-11	1.92E-11	1.84E-11
276	2.14E-11	1.90E-11	1.82E-11
298	1.83E-11	1.74E-11	1.64E-11
313	1.68E-11	1.66E-11	1.55E-11
323	1.60E-11	1.62E-11	1.50E-11
330	1.55E-11	1.60E-11	1.47E-11
348	1.45E-11	1.55E-11	1.40E-11
350	1.44E-11	1.54E-11	1.39E-11
400	1.26E-11	1.49E-11	1.28E-11
500	1.16E-11	1.56E-11	1.31E-11
600	1.24E-11	1.78E-11	1.46E-11
800	1.68E-11	2.49E-11	1.87E-11
1000	2.46E-11	3.56E-11	2.50E-11
1200	3.62E-11	5.01E-11	3.38E-11
1500	6.16E-11	7.94E-11	5.15E-11
1800	9.96E-11	1.19E-10	7.50E-11
2000	1.33E-10	1.51E-10	9.39E-11